

Kinetic Isotope Effects in Oxygen in the Laboratory Dehydration of Magnesian Minerals[†]

Robert N. Clayton* and Toshiko K. Mayeda[‡]

Enrico Fermi Institute, University of Chicago, Chicago, Illinois 60637

Received: September 29, 2008; Revised Manuscript Received: December 19, 2008

Laboratory studies of vacuum dehydration of Mg–O–H units in minerals and rocks reveal large kinetic isotope effects in oxygen, with light-isotope enrichment in the liberated water, and concomitant heavy-isotope enrichment in the residual solids. Application of the same techniques to a meteorite assemblage including hydrous magnesium silicates shows a much more complex behavior, probably due to isotopic heterogeneity inherited from processes on the meteorite parent body. Measurements of both the ¹⁷O/¹⁶O variations and the ¹⁸O/¹⁶O variations confirm theoretical predictions that slopes of three-isotope correlation lines are systematically larger for equilibrium isotope effects than for kinetic isotope effects.

Introduction

Mass-dependent chemical fractionation of stable isotopes can be divided into two categories:¹ equilibrium and kinetic. In this paper, the term “kinetic isotope effect” is used in the sense discussed by Bigeleisen and Wolfsberg.² Equilibrium isotope effects depend on the free-energy differences between reactants and products in an isotope exchange reaction, and a kinetic isotope effect is the ratio of two rate constants in a reaction involving an isotopic substitution, which is determined by a difference in activation energy, the height of the energy barrier between reactants and the transition state. In a primary kinetic isotope effect, this energy difference is important when the isotopic substitution occurs at an atom that is involved in bond-forming or bond-breaking in the transition state. Unfortunately, in the geochemical literature, the term “kinetic isotope effect” is sometimes used as a general term for failure of an isotopic exchange reaction to reach equilibrium.³

The theory of equilibrium isotope effects was well-established over 60 years ago,^{4,5} and has been amply confirmed experimentally. The theory is very simple in the harmonic oscillator approximation, and for exchange reactions involving only gaseous molecules, it requires only the frequencies of the normal modes of vibration as input data. Furthermore, the temperature dependence is also simple, with $\ln K$ going linearly to zero with T^{-2} (T in Kelvin). Kinetic isotope effects are more complicated, generally dependent on the structure and properties of a “transition state”, which cannot be studied by spectroscopic means.⁶ The magnitude of kinetic isotope effects may be of the same order as that of equilibrium effects, but the temperature dependence may differ considerably. For example, Van Hook⁷ states: “simple $1/T$ or $1/T^2$ temperature dependencies are not to be expected except at the temperature extremes”.

Kinetic isotope effects, especially in hydrogen and carbon, have been widely used as probes of organic reaction mechanisms by interpretation of the properties of the transition state. Isotope geochemistry, on the other hand, has been based primarily on equilibrium isotope effects, such as liquid–vapor fractionation of meteoric waters,⁸ and carbonate–water fractionation in seawater.⁹ Terrestrial geochemical processes are usually of sufficient duration to allow a close approach to an equilibrium

distribution of stable isotopes among phases. Kinetic isotope effects may occur in chemical processes that involve interaction between gaseous molecules and condensed phases, in which the processes may be rapid and unidirectional. A notable example is the evaporation of solid minerals or melts into the vacuum of space in the early solar system. In such cases, kinetic isotope effects are the dominant fractionation mechanism. An example, well studied in the laboratory, with direct application to meteoritic materials, is the isotopic fractionation of oxygen, magnesium, and silicon in the vacuum evaporation of magnesium silicate melts.¹⁰

There are also geochemically important analytical procedures that involve kinetic isotope effects. The best known of these is the decomposition of carbonate minerals to yield carbon dioxide for mass spectrometry, either by reaction with acid¹¹ or by thermal decomposition.¹² In the carbonate ion, all three C–O bonds are chemically equivalent. Releasing CO₂ from carbonates requires breaking of a C–O bond, which is faster for a weaker ¹²C–¹⁶O bond than for a stronger ¹²C–¹⁸O bond, so that the product CO₂ is enriched in the heavier isotopes of oxygen relative to the reactant carbonate. At room temperature, this enrichment is about 1% in the ¹⁸O/¹⁶O ratio¹² (or 10–11 permil (‰) in the conventional notation), with a second-order dependence on the metal cation of the carbonate.¹³ By coincidence, the value of this fractionation factor at 25 °C is similar to the equilibrium fractionation of oxygen isotopes between CO₂ and calcite at the same temperature. However, the two processes have different temperature dependence, as illustrated in Figure 1. In Figure 1, the equilibrium curve was calculated by Chacko et al.,¹⁴ the kinetic curve was derived experimentally by Böttcher.¹³

This paper presents experimental data on kinetic isotope effects in oxygen accompanying thermal vacuum dehydration in three increasingly complex systems. The simplest case is the dehydration of brucite [Mg(OH)₂], in which all of the original oxygen atoms are structurally equivalent, and presumably uniform in isotopic composition. The second case is the dehydration of serpentine [Mg₃Si₂O₅(OH)₄], the structure of which can be described as alternating brucite layers and layers of linked SiO₄ tetrahedra, so that there are two chemically different oxygen positions, and only 2/9 of the oxygen atoms are removed by dehydration. The third case is the dehydration of a CM2 carbonaceous chondrite meteorite, Murchison, which

[†] Part of the “Max Wolfsberg Festschrift”.

* Address correspondence to this author.

[‡] Deceased, February, 2004.

contains a serpentine-like hydrous phase, but also contains carbonates and organic compounds that contribute to the volatile products on heating. In all these cases, water is liberated from Mg–O–H units by breakage of Mg–O and O–H bonds, favoring the light isotopes in the evaporated water, and leaving a solid residue enriched in the heavy isotopes. Such a dehydration of meteoritic material in nature should result in enrichment of the heavy isotopes of oxygen, as is seen in a group of “metamorphosed carbonaceous chondrites”.

Even in the apparently simple reaction of dehydration of brucite, the mechanism can be complicated,¹⁵ and kinetic isotope effects have not been calculated theoretically. In this reaction, in order to liberate a water molecule, three Mg–O bonds and one O–H bond are broken,¹⁶ a new O–H bond is formed, and the water molecule diffuses out of the crystal. All of these steps may have isotope effects.

Measurements of the abundances of all three stable isotopes of oxygen may be useful in distinguishing between equilibrium and kinetic isotope effects, based on the relative magnitudes of ¹⁷O/¹⁶O fractionations and ¹⁸O/¹⁶O fractionations. In the high-temperature limit, the ratio of equilibrium 17/16 to 18/16 fractionations reduces to the expression:¹⁷

$$\frac{\ln(Q^{17}/Q^{16})}{\ln(Q^{18}/Q^{16})} = \frac{(1/m_{16} - 1/m_{17})}{(1/m_{16} - 1/m_{18})}$$

where the Q 's are reduced partition functions, and the m 's are atomic masses. For the three isotopes of oxygen, this ratio is 0.5305. Values of the fractionation ratio depend on the substances and processes involved: for terrestrial silicate rocks and minerals, three recent studies^{18–20} indicate that a value of 0.524 applies, except under ultrametamorphic conditions, and for terrestrial rain and snow, Li and Meijer²¹ and Landais et al.²² give 0.528. It should be emphasized that these ratios are not universal constants, but depend on temperature and the substances and reactions involved.

Young et al.²³ have discussed the values of the fractionation ratios for kinetic processes, and give as an end-member approximation:

$$\frac{\ln \alpha(17/16)}{\ln \alpha(18/16)} = \frac{\ln(m_{16}/m_{17})}{\ln(m_{16}/m_{18})}$$

where m 's may be atomic, molecular, or reduced masses. If m is taken to be the mass of a water molecule, the ratio is 0.5142. In this example, and in general, the ratio is smaller for kinetic processes than for equilibrium processes by a measurable amount. In the experiments described in this paper, the two oxygen isotope ratios (¹⁷O/¹⁶O and ¹⁸O/¹⁶O) were measured for both the evolved water and the residual solids, so that the slope of a three-isotope graph of δ^{17} vs δ^{18} (in the logarithmic notation^{18,24}) gives a measure of the ratio for the kinetic processes.

Experimental Methods

Three mineral or rock samples were thermally dehydrated with use of the same apparatus and techniques. The first sample was a museum-quality brucite from Wood's Chrome Mine at Texas, PA.²⁵ The second was derived from the serpentinized peridotite OM5, from the Semail ophiolite in Oman.²⁶ The serpentine-rich sample was produced by flotation in a liquid with specific gravity of 2.80, in order to remove the denser anhydrous phases, olivine and pyroxene. The third sample was an interior piece of the Murchison meteorite, crushed and ground, but not otherwise treated.

The dehydration apparatus was constructed entirely of Pyrex glass, consisting of a horizontal tube, heated externally by a furnace, and an adjacent cold-trap that was at liquid nitrogen temperature during dehydration experiments. The apparatus was attached to a diffusion-pumped vacuum system, providing a vacuum of 10^{-5} Torr before heating. Dehydration of the monomineralic brucite was done in duplicate runs at 300 °C. Serpentine dehydration was also done in duplicate, at successively higher temperatures from 100 to 600 °C. A portion of the solid phase was removed after each heating step for isotopic analysis. The procedure for Murchison was essentially the same as that for serpentine, except that an additional step at 700 °C was included, and an attempt was made to quantify the yield of CO₂ liberated at higher temperatures. Oxygen isotopic

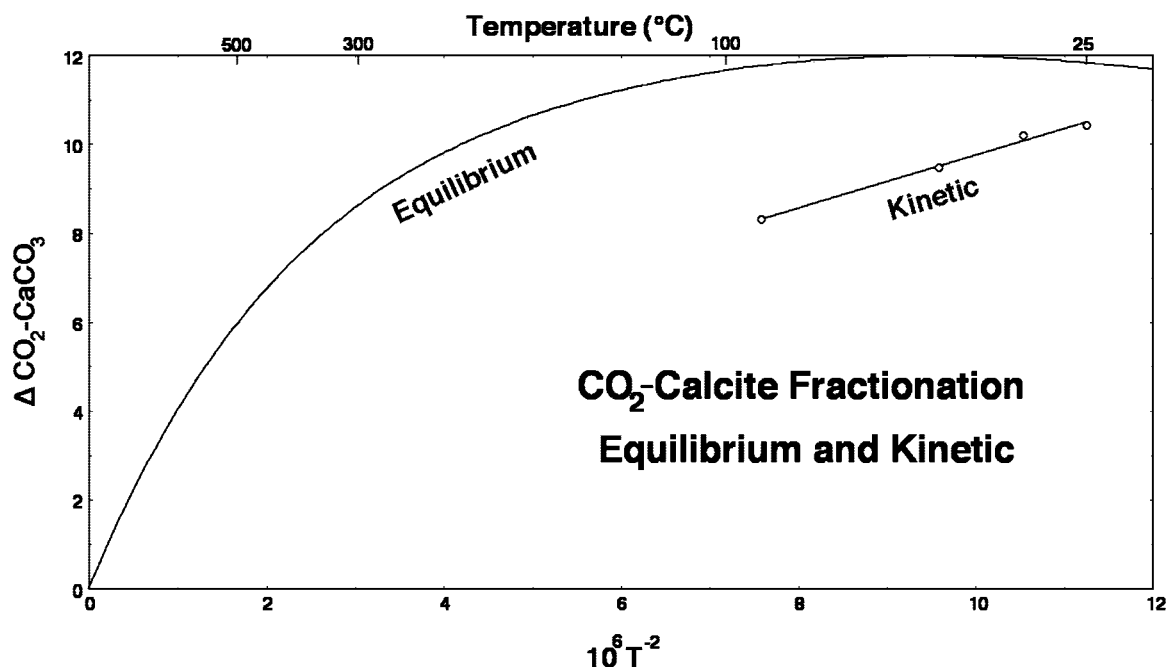


Figure 1. Temperature dependence of ¹⁸O/¹⁶O fractionation between CO₂ and CaCO₃ at equilibrium¹⁴ and on acid liberation of CO₂.¹³

TABLE 1: Brucite Dehydration

run no.	sample (mg)	temp (°C)	time (h)	% dehydr	$\delta^{18}w^a$	$\delta^{17}w$	$\delta^{18}p$	$\delta^{17}p$	$\delta^{18}b$	$\delta^{17}b$	Δ^{18}_{w-b}	Δ^{17}_{w-b}	θ
1	37.6	300	23	82.7	-25.02	-12.96	5.42	2.53	-9.80	-5.21	-15.49	-7.82	0.505
2	33.	300	57	80.8	-23.97	-12.20	2.64	1.13	-10.67	-5.54	-13.53	-6.72	0.497

^a δ values in permil relative to SMOW; subscripts w = water, p = periclase (MgO), b = brucite (Mg(OH)₂). θ is ratio of Δ^{17}/Δ^{18} . δ values are calculated from logarithmic δ' values (see text).

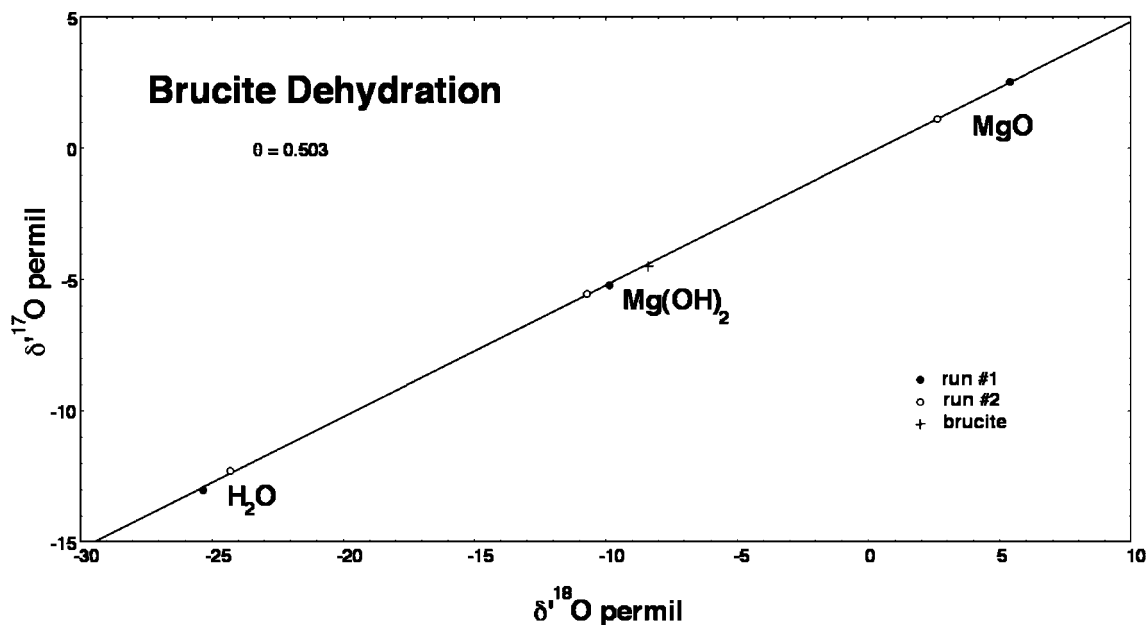


Figure 2. Oxygen three-isotope graph for products of the vacuum dehydration of brucite [Mg(OH)₂] at 300 °C. Data from Table 1. Slope of the kinetic isotope correlation is 0.503. Measured value of the starting material is shown as a + sign.

TABLE 2: OM5 Serpentine Dehydration

run no.	sample (mg)	temp (°C)	time (h)	water (wt %)	$\delta^{18}w^a$	$\delta^{17}w$	$\delta^{18}r$	$\delta^{17}r$	$\delta^{18}mb$	$\delta^{17}mb$	Δ^{18}_{w-r}	Δ^{17}_{w-r}	θ
1	687	25–100	24	0			6.20	3.02					
	663	100–300	119	1.53	-19.76	-10.12	7.34	3.73	6.3	3.2	-27.27	-13.89	0.510
	693	300–440	47	1.31	-18.77	-9.60	8.30	4.16	7.4	3.7	-27.21	-13.80	0.507
	612	440–600	72	3.03	-17.07	-8.70	10.20	5.31	8.1	4.2	-27.37	-14.03	0.513
2	115	25–100	24	0			6.30	3.13					
	105	100–300	109	2.96	-19.78	-9.96	7.34	3.76	5.8	3.0	-27.29	-13.76	0.504
	98	300–440	63	2.04	-18.48	-9.43	8.43	4.23	7.3	3.7	-27.05	-13.76	0.506
	89	440–600	96	3.15	-17.00	-8.59	10.17	5.23	8.2	4.2	-27.26	-13.84	0.508

^a δ values in permil relative to SMOW; subscripts w = water, r = rock, mb = material balance. θ is the ratio of Δ^{17}/Δ^{18} .

analyses of water and residual rock were done by fluorination with bromine pentafluoride to produce O₂, followed by mass spectrometric analysis with standard procedures.²⁷ As will be discussed below, correction of the intensity of the *m/e* 33 peak due to tailing of the large *m/e* 32 peak may have been underestimated.

Results and Discussion

Results of the brucite experiments are given in Table 1. The δ values of water (w) and solid residues (p) are the measured values; the values of the initial brucite were calculated from the measured yields; a direct measurement of the starting material was also made, and is shown in Figure 2. Figure 2 is a three-isotope plot of the data for initial and final phases. In Figure 2 and subsequent three-isotope plots, the logarithmic form of δ was used, $\delta' = 1000 \ln(1 + \delta/1000)$, in order that isotopic fractionation relations are linear.^{18,24}

There is a large mass-dependent kinetic isotope effect in the dehydration process, with heavy-isotope depletion in the evaporated water, relative to the initial brucite, as expected, and

with concomitant enrichment in heavy isotopes in the solid residue. The fractionation in the ¹⁸O/¹⁶O ratio is about 15‰, which is relatively large at 300 °C. The slope of the three-isotope correlation is 0.503, considerably smaller than an equilibrium value. Results similar to ours were obtained for brucite heated slowly over a period of several hours,²⁸ but kinetic isotope effects were reduced to zero if the sample was heated above 500 °C in a few minutes. Even for a reaction that appears simple, the detailed mechanism may be complicated,¹⁵ so that isotope effects may vary with reaction mechanisms.

Results of the serpentine experiments are given in Table 2. The two separate runs produced almost identical results. A test for the quality of the data is the calculation of an isotopic material balance at each heating step. The measured isotopic compositions of water and residue, combined with the measured oxygen yields, allow calculation of the isotopic composition of the starting material at each step. This should correspond to the composition of the solid product of the previous heating step. Thus the entry under “mb” in each row should be compared with the measured values of δr in the previous row. The

TABLE 3: Murchison Dehydration

sample (mg)	temp (°C)	time (h)	water (wt %)	$\delta^{18}\text{w}^a$	$\delta^{17}\text{w}$	$\delta^{18}\text{r}$	$\delta^{17}\text{r}$	$\delta^{18}\text{mb}$	$\delta^{17}\text{mb}$	$\Delta_{\text{w-r}}^{18}$	$\Delta_{\text{w-r}}^{17}$	θ
476	25–100	24	1.49	−9.18	−4.74	+6.97	+0.56	+6.4	+0.4	−16.17	−5.31	0.328
440	100–300	120	5.52	−9.34	−5.48	+9.12	+1.71	+6.6	+0.7	−18.46	−7.21	0.391
400	300–440	46	1.25	−14.46	−8.10	+9.62	+1.59	+8.9	+1.3	−24.14	−9.72	0.403
378	440–600	72	1.05	−7.77	−4.92	+10.80	+2.27	+10.3	+2.1	−18.54	−7.20	0.388
337	600–700	42	0			+10.95	+2.23					

^a Subscripts the same as in Table 2.

agreement is good, considering the potential uncertainties in all the yield measurements.

It may be surprising that the isotopic fractionation between liberated water and residual rock is considerably larger for serpentine dehydration than for brucite dehydration. It is likely that this is a result of large internal isotopic differences between oxygen bonded to Mg and H and oxygen bonded to Si, with the latter bonds being stronger²⁹ and thus enriched in the heavier isotopes. If so, this difference was probably inherited from the original formation of serpentine in nature, and represents an equilibrium isotope effect. If it is assumed that there is a kinetic isotope effect in the dehydration process with a magnitude of 15‰ in $^{18}\text{O}/^{16}\text{O}$, as seen in brucite dehydration, it is estimated that the $\delta^{18}\text{O}$ of the four oxygen atoms per formula unit bonded to Mg and H was about -4% : $(-19 + 15)$.^{29,30} Material balance then allows the calculation of $\delta^{18}\text{O}$ of the remaining five oxygen atoms per formula unit: $5\delta + 4(-4) = 9(+6.3)$, from which $\delta = +14.5\%$. Thus there appears to be an “internal fractionation” between different crystallographic sites of about 19‰ in $\delta^{18}\text{O}$. The published dehydration studies²⁸ were aimed at the use of this internal fractionation for single-mineral isotopic thermometry, so that dehydration conditions were sought that minimized the kinetic isotope effect.

A measure of the “tightness” of oxygen bonding in minerals is the “anion site potential” of Smyth.²⁸ Correlation of this property with heavy-isotope enrichment has been shown.²⁹ From the data of Smyth for the lizardite form of serpentine, the difference in site potential between the four OH oxygens and the five SiO oxygens is 3.87 V. From the correlation between the site potential difference and oxygen isotope fractionation,^{30,31} the internal fractionation can be approximated by:

$$1000 \ln K(18/16) = (3.04 \times 10^6) T^{-2}$$

For $K = 1.019$, this yields $T = 400$ K for the formation temperature of the Oman serpentine, within the existing range of estimates for serpentinization processes. This should not be taken as an independent estimate of the temperature of serpentine formation, but as qualitative evidence for intramineral isotopic fractionation. In their experiments with kaolinite, Girard and Savin²⁸ found a fractionation factor of 1.027 between nonhydroxyl oxygen and hydroxyl oxygen in kaolinite.

A three-isotope plot of all our experimental data for serpentine dehydration is shown in Figure 3, in which the measured slope is 0.507, well below an equilibrium slope. The data points for the two dehydration experiments are indistinguishable from one

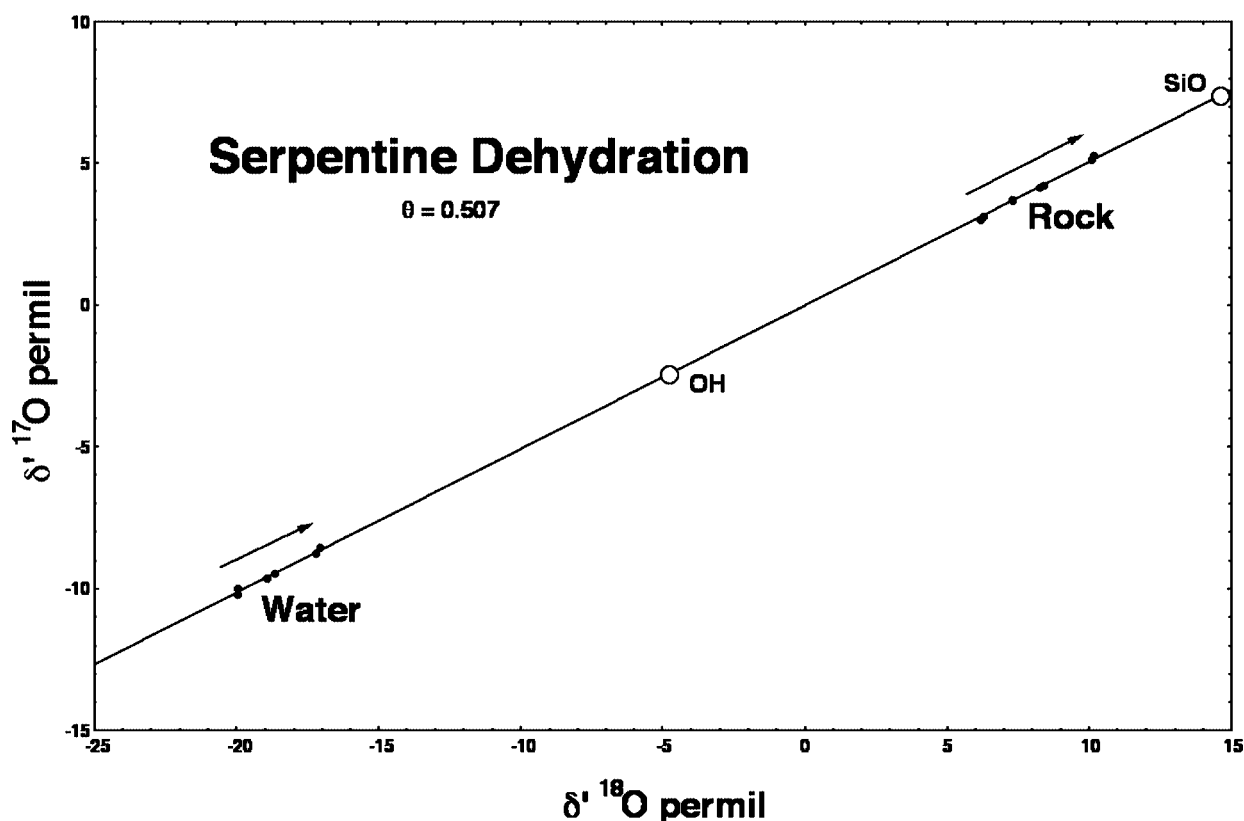


Figure 3. Oxygen three-isotope graph for products of vacuum dehydration of serpentine $[\text{Mg}_3\text{Si}_2\text{O}_5(\text{OH})_4]$ in steps from 100 to 600 °C. Data from Table 2. Slope of the kinetic isotope correlation is 0.507. Arrows indicate the direction of change with increasing dehydration. Estimates of the initial isotopic compositions of OH oxygen atoms and SiO oxygen atoms are also shown.

TABLE 4: Murchison CO₂

sample (mg)	temp (°C)	time (h)	CO ₂ (wt %)	$\delta^{18}\text{O}$	$\delta^{17}\text{O}$	$\Delta^{17}\text{O}$
378	440–600	72	2.0	+19.13	+8.90	-1.05
337	600–700	42	0.9	+19.55	+9.02	-1.15

another. The progressive enrichment in heavy isotopes in the rock residues is much less than that seen in brucite dehydration, since only a few percent of the oxygen was removed, in contrast to 40% in the brucite dehydration.

The results of the dehydration of the Murchison meteorite are given in Table 3. The dehydration procedure followed the same protocol as that for serpentine, in that a sample of the residual solid was taken after each heating step for isotopic analysis. This allowed calculation of a material balance for each step, so that the calculated composition of water plus rock, at each stage, should equal the measured rock composition of the previous stage. The agreement here is not quite as good as that for the serpentine experiment, since other minor oxygen-bearing substances, such as CO₂, were produced, but not included in the mass-balance calculation. The CO₂ liberated at low temperatures contained too much organic contamination for accurate isotope analysis. CO₂ fractions liberated at 600 and 700 °C were converted to O₂ by fluorination, and their oxygen isotope analyses are shown in Table 4. The δ values are not as positive as would be expected for CO₂ derived only from carbonate decomposition, and presumably represent a mixture derived both from carbonates and from oxidation of organic matter. If they had been included in the mass-balance calculations, agreement would have improved.

It has been proposed that oxygen isotopic analysis of water liberated from phyllosilicates in carbonaceous chondrites could allow determination of $\Delta^{17}\text{O}$ (defined as $\delta^{17}\text{O} - 0.52 \delta^{18}\text{O}$) of the aqueous fluid that produced those minerals on the meteorite parent body.³² The values of $\Delta^{17}\text{O}$ are not constant with progressive dehydration, since there are several hydroxyl-bearing minerals in Murchison, with expected different isotopic compositions. Baker et al.³² present data on both $\Delta^{17}\text{O}$ and δ values for water liberated from Murchison by heating. Our data and theirs agree for $\Delta^{17}\text{O}$, in giving a value on the terrestrial fractionation line ($\Delta = 0$) for the 25–100° fraction (probable terrestrial contamination), and Δ values ranging from -0.5‰

to -1.0‰ for higher temperature extractions. This value of Δ may indeed represent that of the serpentine-like minerals from which the water was produced, but cannot represent the value of the water on the parent body, since the hydration process itself derived oxygen both from the aqueous phase and from the precursor anhydrous phases, which typically have much more negative Δ values. Simple mass-balance calculations³³ have shown that Δ values of the aqueous phase responsible for parent-body hydration were much more positive than those in the hydrous minerals today.

A further difference between our water analyses and those of Baker et al.³² is seen in the values of $\delta^{18}\text{O}$ and $\delta^{17}\text{O}$: Baker et al. gave values of $\delta^{18}\text{O}$ of about +8‰, whereas our results average about -10‰, as expected from the kinetic isotope fractionation that we observed in brucite and terrestrial serpentine. Our meteorite samples were about 100 times larger than those of Baker et al., and our analyses were done by dual-inlet mass spectrometry, whereas the analyses of Baker et al. were done by a continuous-flow technique. The reason for the difference in results is unknown.

Figure 4 is a three-isotope plot for our Murchison experiments. Lines shown for reference are the following: TF (terrestrial fractionation) and MAM (Murchison anhydrous minerals), which differs slightly from the usual CCAM (carbonaceous chondrite anhydrous minerals reference line). A line connecting the water analyses and those of the solid residues has a slope of 0.386, indicating clearly that these two reservoirs were not in equilibrium with one another. That is not surprising, since the solid residues contain about 50% unaltered anhydrous olivine and pyroxene, with compositions along the MAM line and with negative Δ values. What is significant in this plot is the progressive increase in δ values of the residues with increasing dehydration (as was seen in terrestrial serpentine dehydration). In our data, this shift amounts to about 4‰ in $\delta^{18}\text{O}$. Thus, the isotopic evolution of carbonaceous chondrite material has two stages of heavy-isotope enrichment: the first due to low-temperature hydration reactions to produce hydrous silicates from olivine and pyroxene (from A to H in Figure 4), possibly followed by a higher temperature dehydration (from H to M in Figure 4). The first process is probably a consequence of the existence of two oxygen reservoirs in the early solar

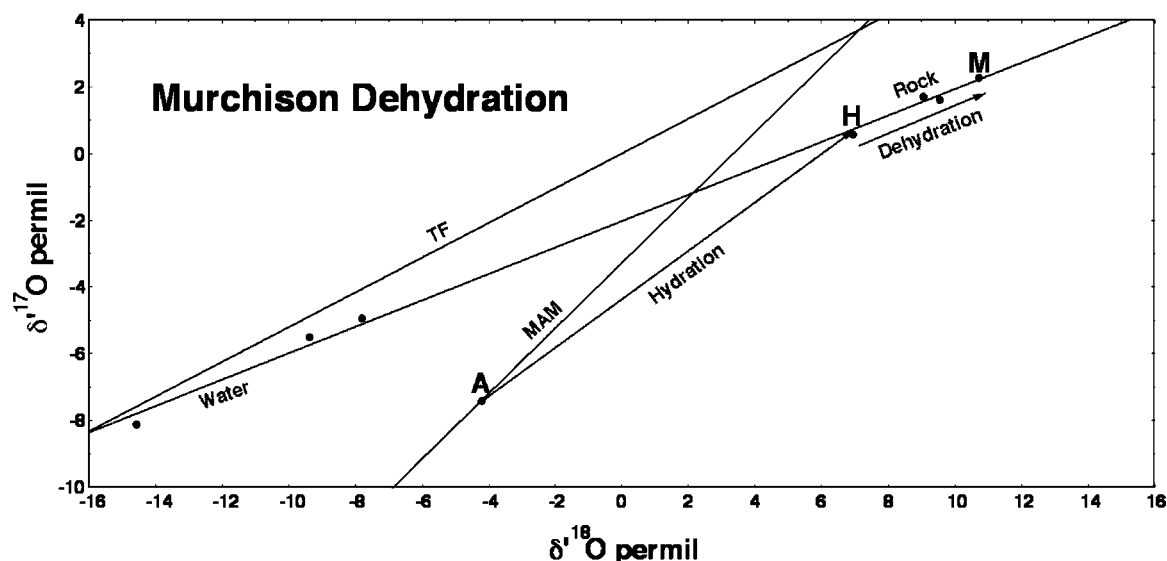


Figure 4. Oxygen three-isotope graph for products of the vacuum dehydration of the Murchison carbonaceous chondrite in steps from 100 to 700 °C. Data from Table 3. Reference lines are the following: TF = Terrestrial fractionation; MAM = Murchison anhydrous minerals.²⁷ Isotopic composition of bulk Murchison is H; composition of anhydrous minerals (mostly olivine and pyroxene) is A; result of dehydration is M.

system: a ^{16}O -rich solid from nebular condensation, and a ^{16}O -poor gas probably produced by photochemistry of CO in the nebula.³⁴ The second process is a kinetic isotope effect of dehydration into the vacuum of space. The principal evidence that this sometimes occurs in nature is the existence of a group of meteorites known as “metamorphosed carbonaceous chondrites”, which are characterized by evidence of thermal decomposition of hydrous silicates.³⁵ They form a separate cluster in an oxygen isotope diagram, enriched in ^{18}O and ^{17}O along a mass-dependent fraction line relative to CI carbonaceous chondrites. Although they constitute a small fraction of known meteorites, reflectance spectra of many asteroids imply that such rocks are common on asteroid surfaces.³⁶

Conclusions

The mass-dependent fractionation of oxygen isotopes in geochemistry occurs in both equilibrium and kinetic processes. The former have been widely exploited by geochemists, but the latter have not, since they are rarely of importance in terrestrial geochemistry, with the notable exception of atmospheric O_2 . The use of kinetic isotope effects in oxygen for elucidation of laboratory reaction mechanisms has been limited by the analytical problems associated with precise mass spectrometry of oxygen. In early solar system chemistry, evaporation and condensation of minerals and melts were common, and produced significant kinetically controlled fractionation of isotopes of major rock-forming elements, such as oxygen, magnesium, silicon, sulfur, calcium, and iron. Precise isotopic measurement of the metallic elements has become possible with the advent of multicollector inductively coupled plasma techniques.³⁷

Multi-isotope analysis is helpful in distinguishing the results of equilibrium and kinetic processes, due to small differences in the mass-dependence. For oxygen isotopes, equilibrium processes have been found to give ratios of $^{17}\text{O}/^{16}\text{O}$ to $^{18}\text{O}/^{16}\text{O}$ fractionations ranging from 0.524 to 0.530. Kinetic processes studied here give ratios of 0.503 to 0.514. Ratios near 0.510, reported in Figures 2 and 3, may be systematically low due to undercorrection for the mass-spectrometric interference of the large “tail” at m/e 32 on the very small peak at m/e 33. A three-isotope plot of 55 terrestrial rock and mineral samples, analyzed by the same techniques and same mass spectrometer as all analyses in this paper, gave a slope of 0.522, compared to the value of 0.524 reported for rock analyses on more modern spectrometers.^{18–20} These slopes could be brought into agreement if the Chicago values of δ^{17} were increased by 0.4%.

Acknowledgment. This research was supported by grants from the U.S. National Science Foundation.

References and Notes

- (1) Wolfsberg, M. *Annu. Rev. Phys. Chem.* **1969**, *20*, 449.
- (2) Bigeleisen, J.; Wolfsberg, M. *Adv. Chem. Phys.* **1958**, *1*, 15.
- (3) McConnaughey, T. *Geochim. Cosmochim. Acta* **1989**, *53*, 151.
- (4) Bigeleisen, J.; Mayer, M. G. *J. Chem. Phys.* **1947**, *15*, 261.
- (5) Urey, H. C. *J. Chem. Soc.* **1947**, 562.
- (6) Melander, L.; Saunders, W. H., Jr. *Reaction Rates of Isotopic Molecules*; Wiley: New York, 1980.
- (7) Van Hook, A. J. In *Isotope Effects in Chemical Reactions*; Collins, C. J., Bowman, N. S., Eds.; ACS Monograph No. 167; American Chemical Society: Washington, DC, 1970; p 1.
- (8) Craig, H. *Science* **1961**, *133*, 1702.
- (9) Urey, H. C.; Lowenstam, H.; Epstein, S.; McKinney, C. R. *Geol. Soc. Am. Bull.* **1951**, *62*, 399.
- (10) Davis, A. M.; Hashimoto, A.; Clayton, R. N.; Mayeda, T. K. *Nature* **1990**, *347*, 655.
- (11) McCrea, J. M. *J. Chem. Phys.* **1950**, *18*, 849.
- (12) Sharma, T.; Clayton, R. N. *Geochim. Cosmochim. Acta* **1965**, *29*, 1347.
- (13) Böttcher, M. E. *Isot. Environ. Health Stud.* **1996**, *32*, 299.
- (14) Chacko, T.; Mayeda, T. K.; Clayton, R. N.; Goldsmith, J. R. *Geochim. Cosmochim. Acta* **1991**, *55*, 2867.
- (15) Balmbra, R. R.; Clunie, J. S.; Goodman, J. F. *Nature* **1966**, *209*, 1083.
- (16) Brindley, G. W.; Kao, C.-C. *Phys. Chem. Miner.* **1984**, *10*, 1984.
- (17) Matsuhisa, Y.; Goldsmith, J. R.; Clayton, R. N. *Geochim. Cosmochim. Acta* **1978**, *42*, 173.
- (18) Miller, M. F. *Geochim. Cosmochim. Acta* **2002**, *66*, 1881.
- (19) Rumble, D.; Miller, M. F.; Franchi, I. A.; Greenwood, R. C. *Geochim. Cosmochim. Acta* **2007**, *71*, 3592.
- (20) Pack, A.; Toulouse, C.; Przybilla, R. *Rapid Commun. Mass Spectrom.* **2007**, *21*, 3721.
- (21) Li, W. J.; Meijer, H. A. J. *Isot. Environ. Health Stud.* **1998**, *34*, 349.
- (22) Landais, A.; Barkan, E.; Luz, B. *Geophys. Res. Lett.* **2008**, *35*, L02709.
- (23) Young, E. D.; Galy, A.; Nagahara, H. *Geochim. Cosmochim. Acta* **2002**, *66*, 1095.
- (24) Hulston, J. R.; Thode, H. G. *J. Geophys. Res.* **1965**, *70*, 3475.
- (25) Palache, C.; Berman, H.; Frondell, C. *Dana's Syst. Mineral.* **1944**, *1*, 636.
- (26) Boudier, F.; Coleman, R. G. *J. Geophys. Res.* **1981**, *86*, 2573.
- (27) Clayton, R. N.; Mayeda, T. K. *Earth Planet. Sci. Lett.* **1983**, *62*, 1.
- (28) Girard, J.-P.; Savin, S. M. *Geochim. Cosmochim. Acta* **1996**, *60*, 469.
- (29) Smyth, J. R. *Geochim. Cosmochim. Acta* **1989**, *53*, 1101.
- (30) Smyth, J. R.; Clayton, R. N. *Eos* **1988**, *69*, 1514 (abstract).
- (31) Chacko, T.; Hu, X.; Mayeda, T. K.; Clayton, R. N.; Goldsmith, J. R. *Geochim. Cosmochim. Acta* **1996**, *60*, 2595.
- (32) Baker, L.; Franchi, I. A.; Maynard, J. M.; Wright, I. P.; Pillinger, C. T. *Lunar Planet. Sci.* **1998**, *29*, abstract no. 1740.
- (33) Clayton, R. N.; Mayeda, T. K. *Earth Planet. Sci. Lett.* **1984**, *67*, 151.
- (34) Clayton, R. N. *Nature* **2002**, *415*, 860.
- (35) Tomeoka, K.; Kojima, H.; Yanai, K. *Proceedings of the Antarctic, Symp. No. 2*; NIPR: Tokyo, Japan 1989; p 55.
- (36) Hiroi, T.; Pieters, C. M.; Zolensky, M. E.; Lipschutz, M. E. *Science* **1993**, *261*, 1016.
- (37) Johnson, C. M.; Beard, B. L.; Albarède, F. *Rev. Mineral. Geochem.* **2004**, *55*, 1.

JP808621N